Cell Research (2010) 20:421-433.

www.nature.com/cr

ORIGINAL ARTICLE

The mitochondrial serine protease HtrA2/Omi cleaves RIP1 during apoptosis of Ba/F3 cells induced by growth factor withdrawal

Lieselotte Vande Walle[1, 2], Ellen Wirawan[1, 2], Mohamed Lamkanfi[3, 4], Nele Festjens[1, 2], Jelle Verspurten[1, 2], Xavier Saelens[1, 2], Tom Vanden Berghe[1, 2], Peter Vandenabeele[1, 2]

[1]VIB, Department for Molecular Biomedical Research, B-9052 Zwijnaarde, Belgium; [2]Department of Biomedical Molecular Biology, Ghent University, B-9052 Zwijnaarde, Belgium; [3]VIB, Department of Medical Protein Research, B-9000 Ghent, Belgium; [4]Department of Biochemistry, Ghent University, B-9000 Ghent, Belgium

Interleukin-3 (IL-3) deprivation of the mouse pro-B cell line Ba/F3 induces cell death that is abrogated by B-cell lymphoma 2 (Bcl-2) overexpression, but remains unaffected by the pan-caspase inhibitor carbobenzoxy-valyl-analyl-aspartyl-[O-methyl]-fluoromethylketone (zVAD-fmk). IL-3 withdrawal causes receptor-interacting protein (RIP)1 cleavage into C-terminal fragments of 30 and 25 kDa, and only cleavage leading to the former was prevented by zVAD-fmk. siRNA experiments demonstrated that generation of the 25-kDa fragment was due to a Bcl-2-modulated release of the mitochondrial serine protease high temperature requirement protein A2 (HtrA2)/Omi. Accordingly, recombinant HtrA2/Omi efficiently cleaved mouse RIP1 *in vitro*, generating fragments matching those observed in IL-3-deprived Ba/F3 cells. The HtrA2/Omi cleavage site in mouse RIP1 was mapped to the intermediate domain and the corresponding N- and C-terminal fragments were impaired in their ability to activate nuclear factor-κB, c-Jun N-terminal kinase and p38 mitogen-activated protein kinase. Interestingly, knockdown of HtrA2/Omi afforded protection against IL-3 withdrawal-induced death in the presence of zVAD-fmk, demonstrating a role for HtrA2/Omi in caspase-independent cell death during growth factor withdrawal by cleaving RIP1.

***Keywords*:** HtrA2/Omi, RIP1, Ba/F3, IL-3, apoptosis

Cell Research (2010) **20**:421-433. doi: 10.1038/cr.2010.18; published online 2 February 2010

Introduction

The transcription factor nuclear factor-κB (NF-κB) protects cells from apoptosis through the transcriptional upregulation of survival-promoting genes [1]. During death receptor-induced apoptosis, the initiator caspase-8 cleaves the serine/threonine kinase receptor-interacting protein (RIP)1 [2-4], a protein required for NF-κB activation in response to tumor necrosis factor (TNF), DNA-damaging agents and the Toll-like receptor (TLR) ligands dsRNA and lipopolysaccharide (LPS) [5-8]. The resulting caspase-8-generated RIP1 fragments are incapable of inducing NF-κB activation, which contributes to death receptor-induced apoptosis [2-4]. Cell death induced by interleukin-3 (IL-3) withdrawal in pro-B cells proceeds through the mitochondrial apoptotic pathway [9-11] and was suggested to involve a caspase-independent mechanism, because the pan-caspase inhibitors carbobenzoxy-valyl-analyl-aspartyl-[O-methyl]-fluoromethylketone (zVAD-fmk) and Boc-D-fmk (benzyloxycarbonyl-Asp(OMe)-fluoromethylketone) failed to prevent cell death and the concomitant loss of mitochondrial mem-

Correspondence: Peter Vandenabeele
Tel: +32 9 3313763; Fax: +32 9 3313609
E-mail: peter.vandenabeele@dmbr.VIB-UGent.be

Abbreviations: Apaf-1 (apoptotic protease activating factor 1); Bcl-2 (B-cell lymphoma 2); Boc-D-fmk (benzyloxycarbonyl-Asp(OMe)-fluoromethyl ketone); CrmA (cytokine response modifier A); DD (death domain); HAX-1 (HS-1-associated protein X-1); HtrA2 (high temperature requirement protein A2); IAP (inhibitor of apoptosis); IBM (IAP-binding motif); ID (intermediate domain); IL-3 (interleukin-3); IMS (intermembrane space); JNK (c-Jun N-terminal kinase); KD (kinase domain); LPS (lipopolysaccharide); MAPK (mitogen-activated protein kinase); NF-κB (nuclear factor-κB); Ped/Pea (phosphoprotein enriched in diabetes/phosphoprotein enriched in astrocytes); RHIM (RIP homotypic interaction motif); RIP (receptor-interacting protein); TLR (Toll-like receptor); TNF (tumor necrosis factor); zVAD-fmk (carbobenzoxy-valyl-analyl-aspartyl-[O-methyl]-fluoromethylketone)

Received 4 December 2009; accepted 9 December 2009; published online 2 February 2010

brane potential [9]. In line with these findings, neither caspase-9 nor Apaf-1 (apoptotic protease activating factor 1) was required for apoptosis induced by IL-3 deprivation, while B-cell lymphoma 2 (Bcl-2) overexpression efficiently prevented cell death induced by IL-3 withdrawal [12]. Accumulating evidence indicates that caspases are not the sole determinants of decisions related to life and death in programmed cell death [13], and that multiple pro-apoptotic factors are released from the mitochondrial intermembrane space (IMS) into the cytoplasm of apoptotic cells [14]. One of these factors is the mitochondrial serine protease high temperature requirement protein A2 (HtrA2)/Omi. In the mitochondrial IMS, the serine protease activity of HtrA2/Omi is required for homeostasis of the organelle [15-16], and inactivating mutations have been associated with neurodegenerative disorders such as Parkinson's disease [17]. However, following an apoptotic trigger, HtrA2/Omi is released into the cytosol [18-22], where it contributes to the regulation of apoptosis in both caspase-dependent and caspase-independent fashions. The N-terminal inhibitor of apoptosis (IAP)-binding motif allows HtrA2/Omi to bind to and consequently inhibit IAP proteins, releasing active caspases from their natural inhibitors [18-22]. In addition, HtrA2/Omi contributes directly to apoptosis as a serine protease by proteolytic degradation of IAP proteins [23], the caspase-8 inhibitor phosphoprotein enriched in diabetes/phosphoprotein enriched in astrocytes (Ped/Pea-15) [24] and the anti-apoptotic protein HAX-1 (HS-1-associated protein X-1) [25].

Here we report that RIP1 is cleaved in IL-3-deprived Ba/F3 cells through both caspase-dependent and caspase-independent mechanisms into two C-terminal fragments of 30 and 25 kDa. While zVAD-fmk inhibited the generation of the 30-kDa fragment, the 25-kDa fragment was generated even in the absence of caspase activity, but required the cytosolic release of the mitochondrial serine protease HtrA2/Omi. siRNA-mediated downregulation of HtrA2/Omi prevented the production of the 25-kDa RIP1 cleavage fragment in IL-3-deprived Ba/F3 cells. *In vitro*, recombinant HtrA2/Omi cleaved mouse ^{35}S-labeled RIP1, generating fragments corresponding to the *in vivo* fragments. We mapped the HtrA2/Omi cleavage site to the intermediate domain (ID) of mouse RIP1 and found that the ability of the cleavage fragments to activate NF-κB was substantially impaired. Furthermore, HtrA2/Omi-mediated RIP1 processing eradicates the RIP1-dependent activation of MAP kinases p38 and c-Jun amino-terminal kinase (JNK) [26-27]. These results indicate that HtrA2/Omi cleaves RIP1 in the mitochondrial apoptotic pathway during IL-3 deprivation, which leads to termination of signaling by NF-κB, p38 mitogen-activated protein kinase (MAPK) and JNK. In this context, the role of HtrA2/Omi resembles that of caspase-8 in death receptor-induced apoptosis [2-4].

Results

Apoptosis of IL-3-deprived Ba/F3 cells depends on the release of mitochondrial factors but not on caspase activity

IL-3 deprivation of Ba/F3 cells induces the apoptotic mitochondrial pathway [10], but the contribution of caspase-independent pathways has not been fully characterized. Apoptosis induced in the mouse pro-B cell line FL5.12 by IL-3 deprivation was reported to proceed through a caspase-independent mechanism [9]. To verify whether apoptosis induced in Ba/F3 cells by IL-3 deprivation proceeds through the mitochondrial pathway, we used Bcl-2 overexpressing Ba/F3 cells. The anti-apoptotic Bcl-2 protein is known to block the mitochondrial apoptotic pathway by preventing the release of mitochondrial pro-apoptotic proteins, such as cytochrome *c* and HtrA2/Omi [28]. Kinetics of Ba/F3 apoptosis in response to IL-3 depletion was determined by measuring DNA hypoploidy (Figure 1A) and plasma membrane permeabilization (Figure 1B). Withdrawal of IL-3 induced apoptosis of Ba/F3 cells in a time-dependent way (Figure 1). As expected and in line with previous reports [10, 12], overexpression of Bcl-2 prevented apoptosis (Figure 1), indicating that apoptosis induced by IL-3 deprivation is mediated through the release of mitochondrial factors. Once mitochondrial proteins are released into the cytosol, both caspase-dependent and caspase-independent pathways are triggered [14]. To investigate the role of caspases downstream of mitochondrial membrane permeabilization in IL-3-deprived Ba/F3 cells, we compared cell death kinetics in the presence and absence of the pan-caspase inhibitor zVAD-fmk. Interestingly, although caspase activity was effectively abrogated (Figure 1C), late membrane permeabilization proceeded and was unchanged in zVAD-fmk-pretreated cells (Figure 1D). In addition, although zVAD-fmk completely abolished caspase-3-like activity (Figure 1C), it was unable to prevent morphological features of apoptosis, such as karyorrhexis and cell shrinkage (Figure 1F), or the molecular parameter of apoptosis, DNA hypoploidy (Figure 1E).

Accumulating evidence indicates that caspases are not the sole determinants of programmed cell death [13]. Besides cytochrome *c*, multiple pro-apoptotic factors are released from the IMS into the cytosol of apoptotic cells [14]. We therefore investigated the release of the mitochondrial pro-apoptotic factors HtrA2/Omi and cytochrome *c* in IL-3-deprived Ba/F3 cells that had been

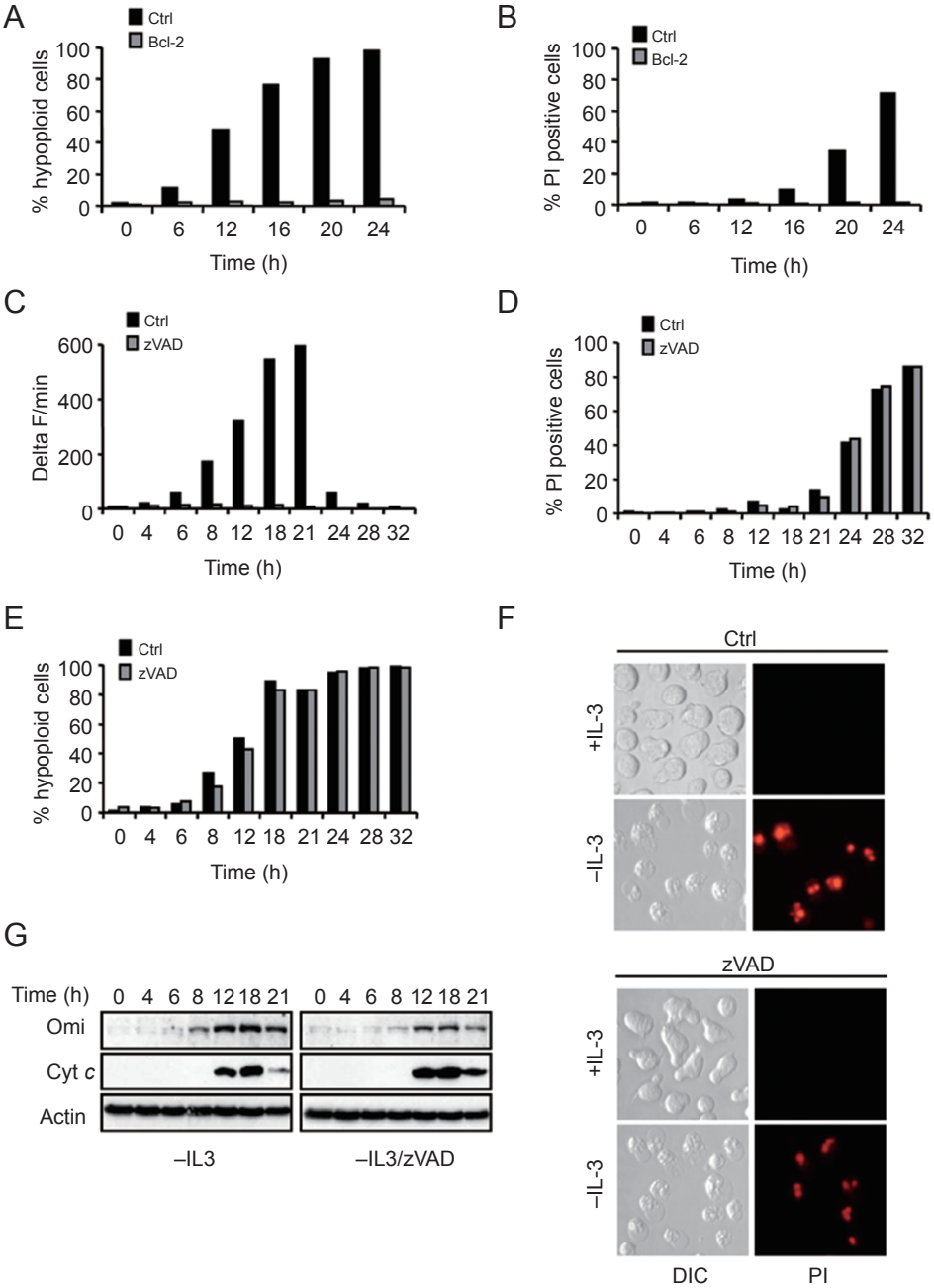

Figure 1 IL-3 deprivation of Ba/F3 cells induces apoptosis through the mitochondrial caspase-independent pathway. **(A-B)** Ba/F3 cells (black bars) and Ba/F3 cells stably overexpressing Bcl-2 (gray bars) were cultured without IL-3 for the indicated times. The percentage of cells containing hypoploid DNA, determined by PI staining after permeabilization by freezing and thawing, was used as a measure of apoptosis **(A)**. Loss of cell membrane integrity was determined as the fraction of PI-positive cells **(B)**. **(C-E)** Ba/F3 cells were either pretreated (gray bars) or not pretreated (black bars) with 50 μM zVAD-fmk and subsequently deprived of IL-3 for the indicated durations. At each time point, the increase in fluorescence intensity per min (ΔF per min) as a result of caspase-mediated Ac-DEVD-amc cleavage was measured **(C)** and the loss of cell membrane integrity was determined by PI uptake **(D)**. The percentage of hypoploid cells, determined by flow cytometry of PI-stained nuclei, was used as a measure of apoptosis **(E)**. **(F)** Ba/F3 cells were left untreated (Ctrl) or were pretreated with 50 μM zVAD-fmk (zVAD) before IL-3 deprivation. Microscopic analysis was done after 24 h of treatment. Note the karyorrhectic nuclei in which nuclear fragmentation appears to have taken place. **(G)** Ba/F3 cells were left untreated (Ctrl) or were pretreated with 50 μM zVAD-fmk (zVAD) and subsequently deprived of IL-3 for the indicated durations. The cytosolic extracts were analyzed by immunoblotting with anti-HtrA2/Omi, anti-cytochrome *c* and anti-actin antibodies. Results are representative of three independent experiments.

pretreated with zVAD-fmk. Cytosolic fractions were prepared at various intervals after IL-3 withdrawal and immunoblotted to detect the cytosolic presence of HtrA2/Omi and cytochrome *c*. HtrA2/Omi and cytochrome *c* were not present in the cytosol of unstimulated control cells, but a time-dependent translocation of both HtrA2/Omi and cytochrome *c* into the cytosol was apparent as early as 8 h after IL-3 deprivation (Figure 1G). In line with the activation of caspases downstream of mitochondrial membrane permeabilization during growth factor depletion, pretreatment of Ba/F3 cells with zVAD-fmk did not affect the release of HtrA2/Omi and cytochrome *c* (Figure 1G). Taken together, these results demonstrate that cell death of Ba/F3 cells induced by IL-3 deprivation is modulated by Bcl-2 but proceeds in the absence of caspase activity.

Caspases are not required for cleavage of RIP1 in response to IL-3 withdrawal

The initiator caspase-8 cleaves the serine/threonine kinase RIP1 during death receptor-induced apoptosis and abrogates NF-κB activation, hence contributing to the sensitization of death receptor-induced apoptosis [2-4]. However, RIP1 cleavage in response to stimuli that induce apoptosis through the mitochondrial death pathway has not been reported. Therefore, we analyzed cleavage of RIP1 after initiation of the mitochondrial pathway in Ba/F3 cells by depriving them of IL-3. A time-dependent decrease of full-length RIP1 in IL-3-deprived Ba/F3 cells occurred ~8 h after stimulation, whereas the loading control remained unchanged (Figure 2A). The disappearance of full-length RIP1 was associated with an increase in RIP1 cleavage fragments (Figure 2A). An antibody

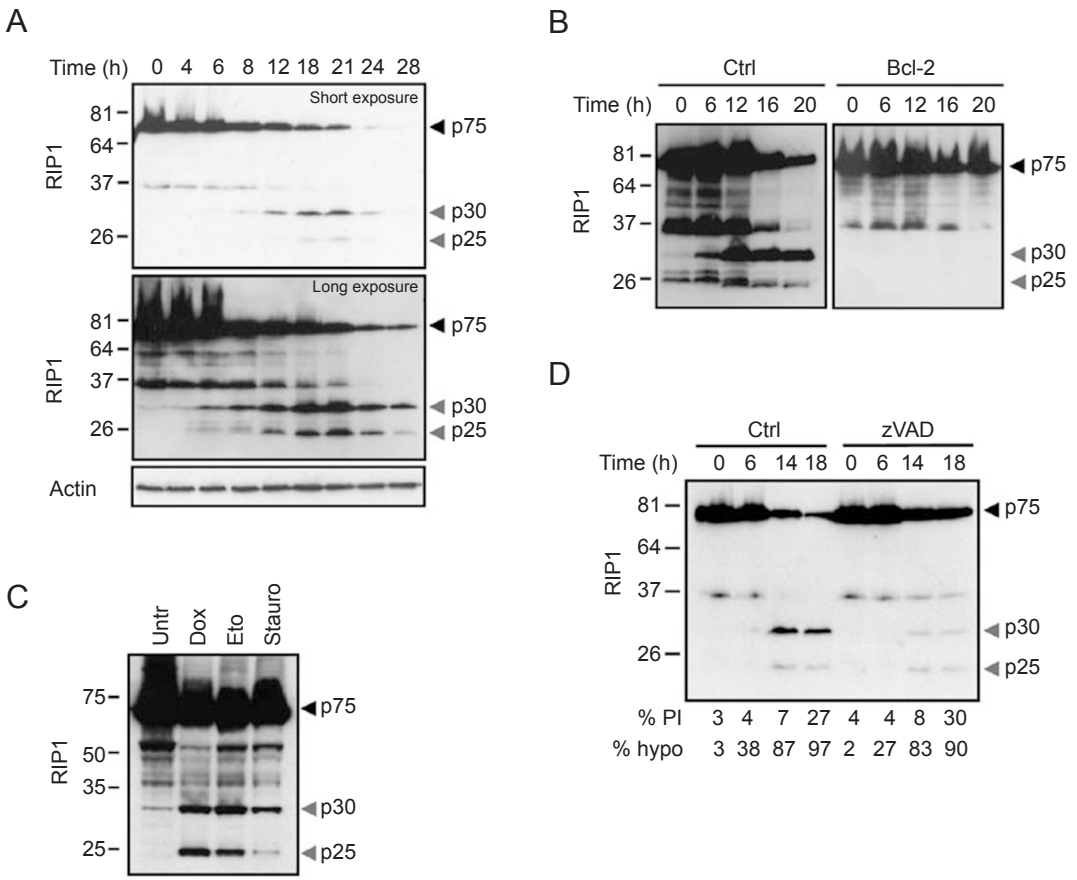

Figure 2 Caspases are not required for cleavage of RIP1 in response to IL-3 withdrawal. **(A)** Total lysates were prepared from untreated or IL-3-deprived Ba/F3 cells at the time indicated and immunoblotted with anti-RIP1 or anti-actin. **(B)** Total lysates of Ba/F3 cells (Ctrl) and Ba/F3.Bcl-2 cells (Bcl-2) deprived of IL-3 for the indicated times were immunoblotted with anti-RIP1 antibody. **(C)** Ba/F3 cells were left untreated or treated with 10 μg/ml doxorubicin, 40 μM etoposide or 1 μM staurosporine. After 20 h, total cell lysates were prepared and immunoblotted with anti-RIP1. **(D)** Ba/F3 cells were left untreated (Ctrl) or were pretreated with 50 μM zVAD-fmk (zVAD) before IL-3 deprivation and then analyzed for RIP1 cleavage. Induction of apoptosis was determined by measuring the percentage of hypoploid cells, and the loss of cell membrane integrity was determined by PI uptake.

against the C-terminal death domain (DD) of RIP1 revealed cleavage fragments of 25 and 30 kDa on immunoblots (Figure 2A). Consistent with cell death kinetics (Figure 1), RIP1 cleavage was completely inhibited when Bcl-2-overexpressing Ba/F3 cells were deprived of IL-3 (Figure 2B), indicating that cleavage of RIP1 into the 25 and 30-kDa C-terminal fragments occurs downstream of mitochondrial engagement. In this respect, a similar RIP1 cleavage pattern was observed when the mitochondrial pathway was induced by the DNA-damaging agents, doxorubicin or etoposide, or by the protein kinase inhibitor, staurosporine (Figure 2C). As our results indicated that caspases are not needed for cell death induced by growth factor withdrawal (Figure 1), we investigated whether caspases were also dispensable for the cleavage of RIP1. Ba/F3 cells were pretreated with zVAD-fmk before incubation in IL-3-deficient culture medium. As shown in Figure 2D, zVAD-fmk did not prevent the generation of the 25-kDa RIP1 fragment but significantly reduced the production of the 30-kDa fragment, suggesting a role for caspases in the generation of the 30-kDa fragment but not the 25-kDa fragment (Figure 2D). These results demonstrate that during apoptosis induced by IL-3 deprivation, RIP1 is cleaved by both caspase-dependent and caspase-independent mechanisms.

HtrA2/Omi mediates RIP1 cleavage during IL-3 deprivation-induced apoptosis

Generation of the 25-kDa RIP1 fragment and the cytosolic release of the mitochondrial serine protease HtrA2/Omi both proceeded independently of caspases in IL-3-deprived Ba/F3 cells. As the cytosolic release of HtrA2/Omi preceded the cleavage of RIP1, we investigated the role of HtrA2/Omi in RIP1 cleavage following the IL-3 deprivation of Ba/F3 cells. We first investigated whether mouse RIP1 processing is observed upon co-expression of human and mouse HtrA2/Omi in 293T cells. Notably, both mouse and human HtrA2/Omi generated a 25-kDa RIP1 fragment that was immunoreactive with antibodies against the C-terminal V5-tag (Figure 3A and 3B). To further explore the role of HtrA2/Omi in IL-3-deprivation-induced cleavage of RIP1, we made use of siRNAs against HtrA2/Omi to downregulate the endogenous protein expression levels in Ba/F3 cells. As expected, HtrA2/Omi siRNA did not affect the expression of the loading control 14-3-3-γ, and control siRNA oligonucleotides had no effect on HtrA2/Omi or 14-3-3-γ expression (Figure 3C). Immunoblots of IL-3-deprived Ba/F3 cells showed that siRNA-mediated downregulation of HtrA2/Omi specifically abolished the generation of the 25-kDa RIP1 fragment (Figure 3D). In contrast, this fragment was present on immunoblots of Ba/F3 cells that had been pretreated with control siRNA oligonucleotides (Figure 3D). To determine whether HtrA2/Omi was directly responsible for cleavage of RIP1, lysates of untreated Ba/F3 cells and *in vitro* translated mouse RIP1 were coincubated with recombinant HtrA2/Omi, and the resulting cleavage fragments were run next to cell lysates of IL-3-deprived Ba/F3 cells. Immunoblot analysis revealed that recombinant HtrA2/Omi generated a 25-kDa RIP1 fragment in Ba/F3 cell lysates that co-migrated with the endogenous 25-kDa RIP1 fragment of IL-3-deprived Ba/F3 cells (Figure 3E). In addition, recombinant HtrA2/Omi cleaved *in vitro* translated mouse RIP1 to generate a 25-kDa RIP1 fragment similar to that in IL-3-deprived Ba/F3 cells (Figure 3E). As expected, the catalytically inactive S306A HtrA2/Omi mutant did not cleave RIP1, excluding the possibility that a co-purified protease was responsible for the observed cleavage of RIP1. In line with our findings in Figure 2, the 30-kDa RIP1 fragment was present in IL-3-deprived Ba/F3 cells but not in the setups incubated with recombinant HtrA2/Omi (Figure 3E). Taken together, these results indicate that HtrA2/Omi released into the cytosol is directly responsible for the cleavage of RIP1 in IL-3-deprived Ba/F3 cells.

HtrA2/Omi cleaves mouse RIP1 in the ID

RIP1 is a serine/threonine kinase that consists of three structural domains: the N-terminal kinase domain (KD) is separated from the C-terminal DD by the so-called intermediate domain (ID) (Figure 4E). To identify the RIP1 structural domain that harbors the HtrA2/Omi cleavage site, we incubated *in vitro* translated mouse RIP1 deletion mutants with recombinant HtrA2/Omi and analyzed the resulting cleavage fragments by SDS-PAGE and autoradiography. As expected, HtrA2/Omi processed full-length RIP1 to generate the 25-kDa fragment and the respective 50-kDa fragment (Figure 4A). In contrast to RIP1 lacking the KD (ΔKD) or the DD (ΔDD), HtrA2/Omi could not cleave RIP1 in which the ID was deleted (ΔID) (Figure 4A). In line with these results, the single-domain mutant RIP1 ID was readily cleaved by HtrA2/Omi (Figure 4B). These data demonstrate that HtrA2/Omi processes mouse RIP1 in the ID and that the presence of the ID is sufficient for recognition and cleavage by HtrA2/Omi.

Analysis of the molecular mass of the RIP1 and RIP1 ID cleavage fragments generated by HtrA2/Omi suggests that HtrA2/Omi cleaves mouse RIP1 in the L_{451}SWPATQTVWNN$_{462}$ region that precedes the so-called RHIM (RIP homotypic interaction motif) motif in the C-terminus of the RIP1 ID domain. To confirm that this region is critical for HtrA2/Omi-mediated processing of RIP1, we constructed RIP1 mutants in which the

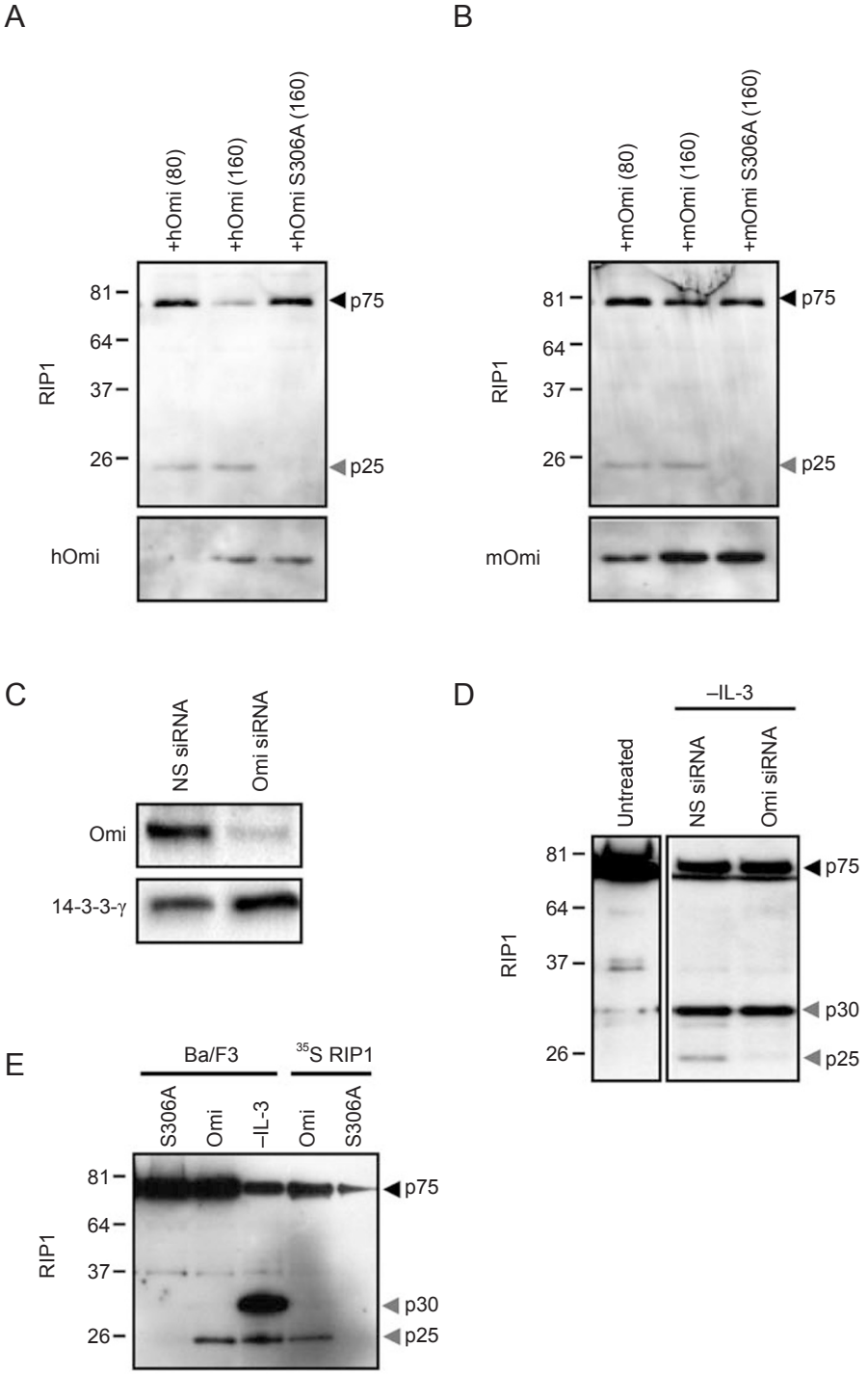

Figure 3 HtrA2/Omi cleaves RIP1 during IL-3 deprivation-induced apoptosis. **(A-B)** Co-transfection of 400 ng expression plasmids encoding C-terminal V5-tagged mouse RIP1 with the indicated concentrations (ng) of plasmids encoding Flag- or E-tagged wild-type or S306A mutant of, respectively, human HtrA2/Omi (**A**, hOmi) or mouse HtrA2/Omi (**B**, mOmi) in 293T cells. After 12 h, total cell lysates were prepared and immunoblotted with anti-V5-tag, anti-Flag-tag or anti-E-tag antibodies. **(C)** Total lysates of Ba/F3 cells transfected with nonspecific (NS) or HtrA2/Omi-specific siRNA were prepared and immunoblotted with anti-HtrA2/Omi or anti-14-3-3-γ antibodies. **(D)** Anti-RIP1 western blot analysis of cellular extracts of untreated or IL-3 depleted Ba/F3 cells that were transfected with either NS or HtrA2/Omi-specific siRNA. **(E)** Ba/F3 cell lysates (Ba/F3) or *in vitro* translated ^{35}S-labeled mouse RIP1 (^{35}S RIP1) were incubated with 100 nM of recombinant HtrA2/Omi S306A or wild-type HtrA2/Omi for 1 h at 37 °C, run in parallel with lysates of Ba/F3 cells deprived of IL-3 for 18 h, and analyzed by immunoblotting with anti-RIP1 antibody.

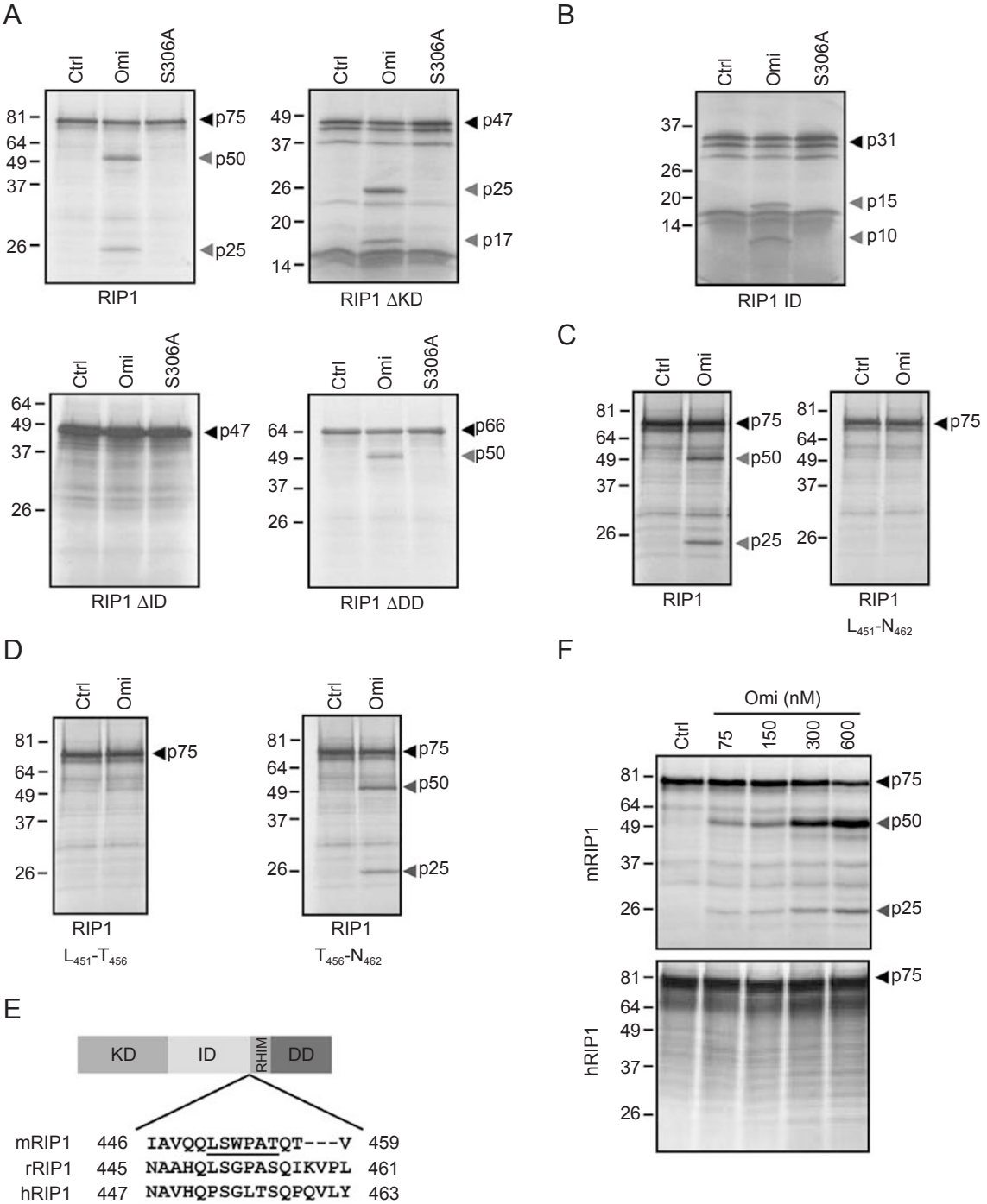

Figure 4 Mapping the HtrA2/Omi cleavage site in mouse RIP1. **(A-B)** *In vitro* translated ^{35}S-labeled wild-type mouse RIP1, RIP1 deletion mutants (ΔKD, ΔID, ΔDD) **(A)** or single-domain mutant RIP1 ID **(B)** were co-incubated with 100 nM of recombinant HtrA2/Omi S306A or wild-type HtrA2/Omi for 1 h at 37 °C. Cleavage fragments were analyzed by SDS-PAGE and autoradiography. **(C-D)** *In vitro* translated ^{35}S-labeled mouse RIP1 and RIP1 mutants in which amino acids L_{451}-N_{462} **(C)**, L_{451}-T_{456} and T_{456}-N_{462} **(D)** were replaced by alanine residues were incubated with 30 nM recombinant HtrA2/Omi for 1 h at 37 °C. Reaction products were analyzed by SDS-PAGE and autoradiography. **(E)** Schematic representation of the domain structure of RIP1 showing three distinct functional domains: the N-terminal kinase domain (KD, aa 1-304), the intermediate domain (ID, aa 304-553) with the RHIM motif (aa 531-551) and the C-terminal death domain (DD, aa 553-656). Sequence alignment of the HtrA2/Omi cleavage site in mouse RIP1 with the corresponding region in rat and human RIP1 is indicated. **(F)** *In vitro* translated ^{35}S-labeled mouse RIP1 or human RIP1 were left untreated or treated with the indicated concentrations of recombinant HtrA2/Omi for 1 h at 37 °C. Autoradiography shows that HtrA2/Omi cleaves mouse RIP1 but not human RIP1.

12 amino-acid residues of this motif were replaced by Ala residues. Replacing this potential cleavage site peptide with Ala residues completely protected RIP1 from cleavage by HtrA2/Omi, showing that the HtrA2/Omi cleavage site is located between Leu_{451} and Asn_{462} (Figure 4C). To identify the cleavage site more precisely, the first six (RIP1 L_{451}-T_{456}) or the last six (RIP1 T_{456}-N_{462}) amino acids of this motif were converted to Ala. Substitution of L_{451}-T_{456} with Ala in wild-type RIP1 abolished the cleavage of RIP1 by HtrA2/Omi (Figure 4D). In line with this result, the RIP1 T_{456}-N_{462} mutant was cleaved by HtrA2/Omi to the same extent as wild-type RIP1 (Figure 4D). All together, these results demonstrate that the HtrA2/Omi cleavage site in mouse RIP1 is located between Leu_{451} and T_{456}. Since this region is not well conserved in human RIP1 (Figure 4E), we compared the efficiency with which human RIP1 and mouse RIP1 were processed by recombinant HtrA2/Omi *in vitro*. Whereas 75 nM HtrA2/Omi efficiently generated 50- and 25-kDa fragments from mouse RIP1, human RIP1 was barely processed even at an HtrA2/Omi concentration of 600 nM (Figure 4F). These results suggest that HtrA2/Omi-mediated cleavage of RIP1 might be a species-specific adaptation that is not conserved in humans.

Cleavage of RIP1 by HtrA2/Omi abolished the NF-κB-inducing activity of RIP1

RIP1 is involved in NF-κB activation in response to different stimuli, including TNF, DNA-damaging agents and the TLR ligands dsRNA and LPS [5-8]. In contrast to full-length RIP1, the cleavage fragments generated by caspase-8 during death receptor-induced apoptosis, when overexpressed in 293T cells, cannot induce NF-κB activation [2-3]. To study whether HtrA2/Omi-mediated cleavage of RIP1 also affects its NF-κB-inducing activity, expression vectors encoding $RIP1_N$ (aa 1-456) or $RIP1_C$ (aa 456-656) were co-transfected with an NF-κB-driven luciferase reporter in 293T cells. Empty vector and plasmids encoding wild-type RIP1 were incorporated in these studies as negative and positive controls, respectively. To prevent RIP1-induced apoptosis, the expression vector of poxvirus protein cytokine response modifier A (CrmA) was also included in the transfection. As expected, wild-type RIP1 potently induced NF-κB activation, while empty vector-transfected cells failed to activate NF-κB (Figure 5A). In contrast to full-length RIP1, the HtrA2/Omi-generated RIP1 fragments could not activate NF-κB effectively. Indeed, the RIP_N fragment showed no activity, whereas the RIP_C fragment induced a much weaker activation of NF-κB (Figure 5A). Western blot analysis of lysates of transfected 293T cells confirmed the appropriate expression of all constructs (Figure 5B).

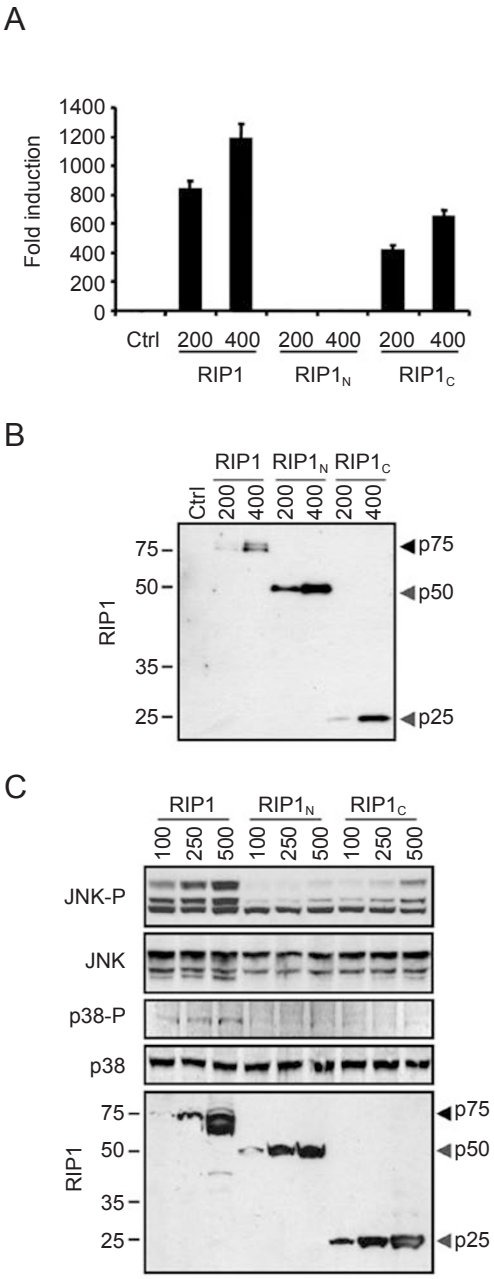

Figure 5 Cleavage of RIP1 by HtrA2/Omi results in the blockage of the activation of NF-κB, p38 MAPK and JNK. **(A)** 293T cells were transiently co-transfected with an NF-κB-driven luciferase reporter plasmid and either empty vector (−) or the indicated amounts (ng) of expression plasmids encoding E-tagged wild-type RIP1, $RIP1_N$ or $RIP1_C$. After 24 h, lysates were analyzed for luciferase activity. **(B)** Aliquots of the same cell lysates were analyzed by SDS-PAGE and immunoblotting using anti-E-tag antibody to confirm the appropriate expression of all constructs. **(C)** 293T cells were transfected with the indicated amounts (ng) of expression plasmids encoding E-tagged wild-type RIP1, $RIP1_N$ or $RIP1_C$. After 24 h, total lysates were analyzed by immunoblotting using anti-JNK, anti-phospo-JNK, anti-p38 MAPK, anti-phospho-p38 MAPK and anti-E-tag antibodies.

In addition to its role in inducing NF-κB activation, RIP1 was reported to be required for TNF-induced activation of JNK and p38 MAPK [26]. Moreover, activation of these kinase pathways by transient expression of RIP1 in 293T cells was shown to be dependent on the RIP1 ID domain [27]. To examine whether HtrA2/Omi-mediated cleavage of RIP1 also affected JNK and p38 MAPK activation, we transiently transfected 293T cells with vectors encoding $RIP1_N$ or $RIP1_C$ in the presence of CrmA and then analyzed them by western blot. In contrast to empty vector-transfected cells, JNK and p38 MAPK were both phosphorylated in 293T cells overexpressing full-length RIP1 (Figure 5C). However, neither the N-terminal nor the C-terminal RIP1 fragment recapitulated the potent ability of full-length RIP1 in activating p38 MAPK and JNK (Figure 5C). Taken together, these results demonstrate that HtrA2/Omi-mediated cleavage of RIP1 affects its ability to induce activation of NF-κB, JNK and p38 MAPK.

HtrA2/Omi siRNA reduces caspase-independent cell death induced by IL-3 withdrawal

To study the role of RIP1 cleavage during cell death induced by growth factor deprivation, we assessed the cell viability of Ba/F3 cells in response to IL-3 withdrawal in the presence of zVAD-fmk and HtrA2/Omi siRNA. Ba/F3 cells were transfected with HtrA2/Omi siRNA or control siRNA, and after 24 h they were treated with zVAD-fmk and then incubated in IL-3-deficient medium. While HtrA2/Omi siRNA decreased the levels of HtrA2/Omi, actin expression was unaffected by any of the siRNA treatments (Figure 6A). Interestingly, unlike treatment with zVAD-fmk (Figure 1), treatment with HtrA2/Omi siRNA rendered Ba/F3 cells more resistant to IL-3 withdrawal-induced cell death than control siRNA-treated cells (Figure 6B). These results demonstrate that HtrA2/Omi, possibly by cleaving RIP1, plays a role in the regulation of caspase-independent cell death in this system.

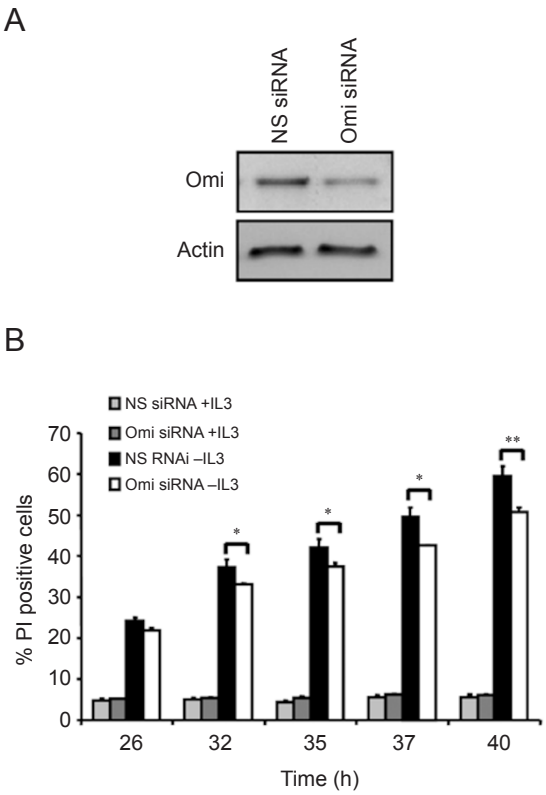

Figure 6 Suppression of HtrA2/Omi decreases caspase-independent cell death. **(A)** Total lysates of Ba/F3 cells transfected with nonspecific (NS) or HtrA2/Omi-specific siRNA were prepared and immunoblotted with anti-HtrA2/Omi or anti-actin antibodies. **(B)** Ba/F3 cells were transfected with NS or HtrA2/Omi-specific siRNA. The next day, cells were pretreated with zVAD-fmk and either left untreated or incubated in IL-3-deficient medium. At the indicated time points, cell death was assessed by cytofluorometric analysis of PI uptake. Data represent the mean ± SD of three independent experiments. **P* < 0.05 and ***P* < 0.01.

Discussion

The bone marrow-derived pro-B cell line Ba/F3 requires IL-3 to proliferate and to overcome the default apoptotic program. Indeed, Ba/F3 cells become committed to apoptosis when deprived of IL-3, and hence multiple signaling pathways downstream of IL-3 have been proposed to prevent apoptosis [29]. For instance, the constitutive activation of NF-κB in the presence of IL-3 is required for the survival of Ba/F3 cells [30-32]. As NF-κB activation is known to protect cells against apoptosis through the transcriptional upregulation of survival-promoting genes [1], it has been proposed that cell fate following growth factor withdrawal is determined by the ability to maintain NF-κB activity [31-33]. In line with this notion, previous studies observed a large decrease in NF-κB activity before the propagation of apoptosis when Ba/F3 cells were deprived of IL-3 [30]. In addition, the executioner caspases-3 and -6 cleave and inactivate the p65 subunit of NF-κB, which results in the enhancement of apoptotic death of endothelial cells that have been deprived of growth factors [33]. Besides NF-κB, the MAP kinases p38 [34] and JNK [35] were demonstrated to be activated upon IL-3 stimulation of hematopoietic progenitor cells. Like NF-κB activation, p38 MAPK activation is involved in the transcriptional activation of numerous anti-apoptotic genes in response to cellular stress [36-

37], while IL-3-mediated activation of JNK is required for the suppression of apoptosis through phosphorylation and inactivation of the pro-apoptotic protein Bad in pro-B lymphocytes [38].

The importance of the serine/threonine kinase RIP1 in hematopoietic cell homeostasis is apparent from RIP1-deficient mice that exhibit decreased peripheral blood lymphocyte counts, suggesting an essential role for this kinase in T- and B-cell survival [7]. Furthermore, RIP1 was shown to be indispensable for the activation of NF-κB in response to TNF in pro-B cells [7], as well as for TNF-induced activation of the MAPKs p38 and JNK [26]. Interestingly, this kinase is proteolytically inactivated by caspase-8 during death receptor-induced apoptosis [2-4]. However, it is not known whether RIP1 is also cleaved in response to triggers that engage the mitochondrial death pathway. Here, we report that apoptosis induced in Ba/F3 cells by IL-3 deprivation proceeds through the mitochondrial pathway, but caspases seem to be dispensable for cell death. Furthermore, apoptosis induced by IL-3 depletion was shown to be associated with the cleavage of RIP1 into two C-terminal fragments of 30 and 25 kDa. Whereas generation of the 30-kDa fragment is prevented by the pan-caspase inhibitor zVAD-fmk, cleavage of RIP1 into the 25-kDa fragment required the cytosolic release of the mitochondrial serine protease HtrA2/Omi. siRNA-mediated knockdown of HtrA2/Omi prevented the generation of the 25-kDa RIP1 cleavage fragment in IL-3-deprived Ba/F3 cells. Moreover, the 25-kDa RIP1 fragment observed in IL-3-deprived Ba/F3 cells co-migrated with a cleavage fragment of RIP1 that was generated by incubating *in vitro* translated mouse RIP1 with recombinant HtrA2/Omi. These results confirm a direct and specific role for HtrA2/Omi in mouse RIP1 processing. Unlike mouse RIP1, human RIP1 was not cleaved by recombinant HtrA2/Omi *in vitro*. This suggests that HtrA2/Omi-mediated cleavage of RIP1 is a species-specific adaptation that is not conserved in humans. Mouse RIP1 deletion mutants were used to map the HtrA2/Omi cleavage site to the region between Leu_{451} and T_{456} in the C-terminal part of the RIP1 ID. Co-transfection of the resulting RIP1 cleavage fragments with an NF-κB reporter demonstrated that HtrA2/Omi-mediated cleavage of RIP1 significantly reduces the ability of RIP1 to induce NF-κB activation. Similarly, cleavage of RIP1 abrogated the ability of RIP1 to induce activation of the MAP kinases JNK and p38. Strikingly, reducing the endogenous level of HtrA2/Omi by RNA interference retards IL-3 deprivation-induced death in Ba/F3 cells in the presence of zVAD-fmk. This finding indicates that HtrA2/Omi plays a substantial role in the caspase-independent death pathway induced by IL-3 withdrawal, possibly by cleaving RIP1.

Overall, we show that the mitochondrial serine protease HtrA2/Omi is rapidly released into the cytosol of IL-3-deprived Ba/F3 cells, where it contributes to cell death through the processing and inactivation of RIP1. These results suggest that the cytosolic release of HtrA2/Omi and the consequent cleavage of RIP1 might abrogate survival signaling mediated by NF-κB and the MAP kinases p38 and JNK, hence enhancing apoptosis in response to growth factor withdrawal. This function of HtrA2/Omi in response to stimuli that engage the mitochondrial apoptotic pathway resembles that of caspase-8 during death receptor-induced apoptosis (Figure 7) [2-4].

Materials and Methods

Plasmids

pEF1-mRIP1-V5/His was constructed by inserting a *Bam*HI-*Xba*I fragment, containing mouse RIP1 cDNA without a termination codon, between the *Bam*HI and *Xba*I sites of pEF1/V5-HisA (Invitrogen, Carlsbad, CA, USA). Mouse RIP1 deletion mutants (ID, ΔKD, ΔID, ΔDD) were generated by PCR using modified complementary PCR adaptor primers and cloned into pEF1/V5-HisA. RIP1 mutants containing Ala cluster substitutions were constructed by site-directed mutagenesis PCR and cloned into pEF1/V5-HisA. cDNA encoding wild-type RIP1, $RIP1_N$ (aa 1-456) or $RIP1_C$ (aa 456-656) was amplified by PCR, and the amplified product was digested with *Not*I and *Bgl*II, and the corresponding fragment was cloned into pCAGGS. pEF1-hRIP1-V5/His was constructed by inserting a *Not*I-*Xba*I PCR fragment, containing human RIP1 cDNA, between the *Not*I and *Xba*I sites of pEF1/V5-HisB. The cDNA encoding mature mouse HtrA2/Omi was amplified by PCR from a full-length cDNA clone of mouse HtrA2/Omi in the pCMV-SPORT6 vector, which was obtained from RZPD (Berlin, Germany). The amplified product was digested with *Not*I and *Bgl*II and cloned in pCAGGS-E in frame with the N-terminal E-tag. cDNA encoding the catalytically inactive S306A mutant of HtrA2/Omi was constructed by site-directed mutagenesis PCR. cDNA encoding the human HtrA2/Omi wild-type or the S306A mutant was amplified by PCR from pEF1-HtrA2/Omi-V5/HisA and pEF1-HtrA2/Omi-S306A-V5/HisA [39], respectively, and the amplified product was digested with *Kpn*I and *Bgl*II and cloned in pCAGGS-Flag in frame with the N-terminal Flag-tag. Plasmid pIgK3conaLUC, encoding the luciferase reporter gene driven by an NF-κB responsive promoter, was a generous gift from Dr A Israel (Institut Pasteur, Paris, France). The pAct-bGal vector, containing the β-galactosidase gene after the β-actin promoter, was obtained from Dr Inoue (Institute of Medical Sciences, Tokyo, Japan), and pCAGGS-CrmA has been described previously [40]. Proper construction of all the plasmids was confirmed by DNA sequencing.

Induction of cell death and FACS analysis

The IL-3-dependent mouse pro-B cell line Ba/F3 was maintained in RPMI 1640 medium (Invitrogen) supplemented with 10% (v/v) heat-inactivated fetal calf serum, penicillin (100 Units/ml), streptomycin (100 μg/ml) and 10% (v/v) conditioned medium

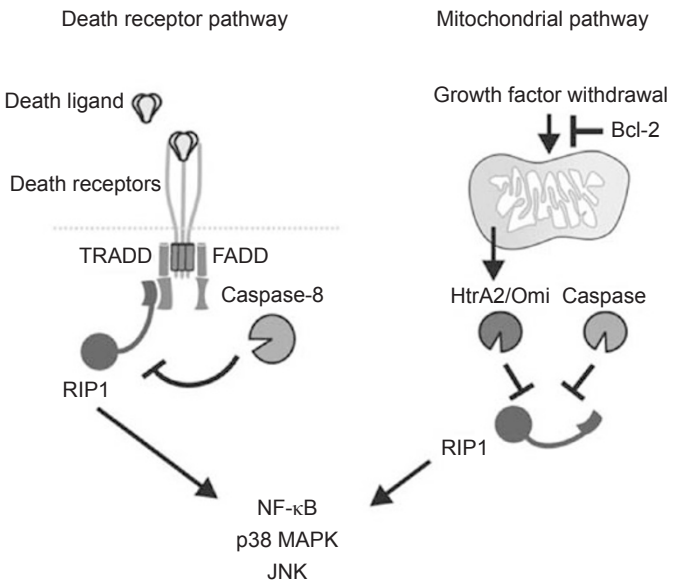

Figure 7 Schematic representation of proteolysis-mediated RIP1 inactivation during apoptosis. When cells undergo death receptor-induced apoptosis, RIP1 is cleaved by caspase-8 to neutralize the protective effect of NF-κB. Here we demonstrate that upon activation of the mitochondrial pathway by growth factor withdrawal, RIP1 cleavage occurs through both caspase-dependent and caspase-independent mechanisms. Caspase-independent cleavage of RIP1 is mediated by the mitochondrial serine protease HtrA2/Omi. HtrA2/Omi-mediated proteolysis of RIP1 eliminates the ability of RIP1 to induce the activation of NF-κB and the MAP kinases p38 and JNK.

from the WEHI-3B cells as a source of mouse IL-3. Ba/F3 cells were stably transfected by electroporation as described previously [41]. Before induction of apoptosis, Ba/F3 cells were resuspended in fresh medium at 3×10^5 cells per ml. The next day, cell death was induced in Ba/F3 cells by IL-3 depletion for different durations and analyzed by monitoring propidium iodide (PI) uptake. PI (30 μM) was added 10 min before measuring and fluorescence was detected at 610 nm on a FACScalibur flow fluorocytometer (Becton Dickinson, Sunnyvale, CA, USA) equipped with a 488-nm argon ion laser. DNA hypoploidy was measured by flow cytometry of PI-stained cells that were permeabilized by freeze thawing. To block caspase activity, cells were pretreated for 0.5 h with 50 μM zVAD-fmk (Bachem, Torrance, CA, USA), washed, and then incubated for the indicated durations in IL-3-deficient medium containing 50 μM zVAD-fmk.

Subcellular fractionation and immunoblot analysis

Ba/F3 cells were washed twice in cold PBS and equal cell numbers were lysed by addition of the Laemmli sample buffer (62.5 mM Tris-HCl pH 6.8, 2% SDS, 10% glycerol, 5% β-mercaptoethanol) and boiling for 10 min. For cytosolic HtrA2/Omi and cytochrome *c* detection, cells were permeabilized in cold cell-free system buffer (10 mM HEPES-NaOH pH 7.4, 220 mM mannitol, 68 mM sucrose, 2 mM NaCl, 2.5 mM KH_2PO_4, 0.5 mM EGTA, 2 mM $MgCl_2$, 5 mM pyruvate, 0.1 mM PMSF, 200 Units/ml aprotinin, 10 mg/ml leupeptin and 10 mM DTT) supplemented with 0.2 mg/ml digitonin and incubated on ice for 1 min. This treatment allows selective lysis of the outer cell membrane without affecting the organelle membranes. Lysates were cleared of cellular debris by centrifugation at 20 000 *g* for 10 min at 4 °C, separated on SDS-PAGE gels of different percentages and transferred into the nitrocellulose membrane by semidry blotting in a buffer containing 25 mM Tris-HCl pH 8.0, 190 mM glycine and 20% methanol. All further incubations were carried out at room temperature on a platform shaker. Blocking, incubation with antibody and washing of the membrane were done in PBS supplemented with 0.02% Tween-20 (v/v) and 3% (w/v) non-fat dry milk. Membranes were incubated with horseradish peroxidase-conjugated secondary antibodies against mouse and rabbit immunoglobulin (Amersham Biosciences, Buckinghamshire, UK). Immuno-reactive proteins were visualized with the enhanced chemiluminescence method (Perkin-Elmer, Boston, MA, USA). The HtrA2/Omi antibody was produced and purified as described previously [39]. Other primary antibodies used were anti-cytochrome *c*, anti-RIP1 (BD Biosciences, San Diego, CA, USA), anti-actin (C-4; MP Biomedicals, Aurora, OH, USA), anti-E-tag (Amersham Biosciences), anti-Flag-tag (Sigma-Aldrich, Bornem, Belgium), anti-14-3-3γ (CG31-2B6, Bio-Connect, Huissen, The Netherlands), anti-p38 MAPK, anti-phospho-p38 MAPK, anti-JNK and anti-phospo-JNK antibodies (Cell Signaling, Danvers, MA, USA).

DEVDase activity

Cells were harvested and lysed in ice-cold caspase lysis buffer (0.05% Nonidet-P40, 220 mM mannitol, 68 mM sucrose, 2 mM NaCl, 2.5 mM KH_2PO_4, 10 mM Hepes pH 7.4, supplemented with 0.1 mM PMSF, 200 Units/ml aprotinin, 10 mg/ml leupeptin and 1 mM oxidized glutathione). Cellular debris was removed by centrifugation, and caspase activity was determined by incubating 10 μl

of the soluble fraction with 50 μM acetyl-Asp(OMe)-Glu(OMe)-Val-Asp(OMe)-aminomethylcoumarin (Ac-DEVD-amc, Peptide Institute, Osaka, Japan) in 200 μl cell-free system buffer. The release of fluorescent 7-amino-4-methylcoumarin was measured for 60 min at 2-min intervals by fluorometry (excitation at 360 nm and emission at 480 nm) (Cytofluor; PerSeptive Biosystems, Cambridge, MA, USA); the maximal rate of increase in fluorescence was calculated (ΔF per min).

In vitro transcription/translation and cleavage assay

Human recombinant HtrA2/Omi and the catalytic inactive S306A mutant of HtrA2/Omi were produced and purified as described previously [39]. Mouse wild-type RIP1 and RIP1 mutants (200 ng) were used as templates for *in vitro*-coupled transcription/translation in a rabbit reticulocyte lysate system according to the manufacturer's instructions (Promega, Madison, WI, USA). To detect the translation products, ^{35}S-methionine was added to the translation reactions. For *in vitro* cleavage, translation reactions (2 μl each) were incubated with recombinant HtrA2/Omi or HtrA2/Omi S306A in a total volume of 24 μl of cell-free system buffer for 1 h at 37 °C. The resulting cleavage products were analyzed by SDS-PAGE and autoradiography.

RNA interference

Transfection experiments were performed using the Amaxa nucleofection technology (Amaxa, Cologne, Germany). Ba/F3 cells (2×10^6) were resuspended in 100 μl Amaxa solution V in the presence of control or HtrA2/Omi siRNA (Dharmacon, Lafayette, CO, USA), and transfected using an electrical setting corresponding to nucleofector program X-01. Cells were then resuspended in prewarmed culture medium at 3×10^5 cells per ml. Forty-eight hours after transfection, cells were depleted of IL-3 and harvested for western blot analysis.

DNA transfection

293T cells were transfected with the indicated expression vectors combined with 100 ng NF-κB-luciferase and pACT-β-galactosidase reporter plasmids. After 24 h, the cells were collected, washed in PBS and lysed in Luciferase lyse buffer (25 mM Tris phosphate pH 7.8, 2 mM DTT, 2 mM CDTA, 10% glycerol and 1% Triton-X-100). On addition of substrate buffer (658 mM luciferin, 378 mM coenzyme A and 742 mM ATP), Luciferase (Luc) activity was assayed in a GloMax 96 Microplate Luminometer (Promega). β-Galactosidase (Gal) activity in cell extracts was assayed with chlorophenol red β-D-galactopyranoside substrate (Roche Applied Science, Basel, Switzerland) and the optical density was read at 595 nm in a Benchmark microplate Reader (Bio-Rad Laboratories, Nazareth, Belgium). Luc values were normalized for Gal values in order to correct for differences in transfection efficiency (plotted as Luc/Gal). The data represent the average ± SD of triplicates.

Conflict of interest

The authors declare no conflict of interest.

Acknowledgments

This work is supported by doctoral grants from the Institute for the Promotion of Innovation by Science and Technology in Flanders (IWT) and the Stichting Emmanuel van der Schueren. Dr Tom Vanden Berghe, Dr Mohamed Lamkanfi and Dr Nele Festjens are paid by a postdoctoral fellowship from FWO (Fonds Wetenschappelijk Onderzoek – Vlaanderen). Research was supported by the Flanders Institute for Biotechnology (VIB) and several grants from the European Union (EC Marie Curie Training and Mobility Program, FP6, ApopTrain, MRTN-CT-035624; EC RTD Integrated Project, FP6, Epistem, LSHB-CT-2005-019067, *APO*-SYS, FP7, HEALTH-F4-2007-200767), the Interuniversity Poles of Attraction-Belgian Science Policy (IAP6/18), FWO (3G.0218.06), and the Special Research Fund of Ghent University (Geconcerteerde Onderzoekstacties 12.0505.02). We thank Dr Amin Bredan (Ghent University) for proofreading the manuscript text.

References

1 Pahl HL. Activators and target genes of Rel/NF-κB transcription factors. *Oncogene* 1999; **18**:6853-6866.
2 Kim JW, Choi EJ, Joe CO. Activation of death-inducing signaling complex (DISC) by pro-apoptotic C-terminal fragment of RIP. *Oncogene* 2000; **19**:4491-4499.
3 Lin Y, Devin A, Rodriguez Y, Liu ZG. Cleavage of the death domain kinase RIP by caspase-8 prompts TNF-induced apoptosis. *Genes Dev* 1999; **13**:2514-2526.
4 Martinon F, Holler N, Richard C, Tschopp J. Activation of a pro-apoptotic amplification loop through inhibition of NF-κB-dependent survival signals by caspase-mediated inactivation of RIP. *FEBS Lett* 2000; **468**:134-136.
5 Cusson-Hermance N, Khurana S, Lee TH, Fitzgerald KA, Kelliher MA. Rip1 mediates the Trif-dependent toll-like receptor 3- and 4-induced NF-κB activation but does not contribute to interferon regulatory factor 3 activation. *J Biol Chem* 2005; **280**:36560-36566.
6 Hur GM, Lewis J, Yang Q, *et al.* The death domain kinase RIP has an essential role in DNA damage-induced NF-κB activation. *Genes Dev* 2003; **17**:873-882.
7 Kelliher MA, Grimm S, Ishida Y, Kuo F, Stanger BZ, Leder P. The death domain kinase RIP mediates the TNF-induced NF-κB signal. *Immunity* 1998; **8**:297-303.
8 Meylan E, Burns K, Hofmann K, *et al.* RIP1 is an essential mediator of Toll-like receptor 3-induced NF-κB activation. *Nat Immunol* 2004; **5**:503-507.
9 Bojes HK, Feng X, Kehrer JP, Cohen GM. Apoptosis in hematopoietic cells (FL5.12) caused by interleukin-3 withdrawal: relationship to caspase activity and the loss of glutathione. *Cell Death Differ* 1999; **6**:61-70.
10 Cornelis S, Bruynooghe Y, Van Loo G, Saelens X, Vandenabeele P, Beyaert R. Apoptosis of hematopoietic cells induced by growth factor withdrawal is associated with caspase-9 mediated cleavage of Raf-1. *Oncogene* 2005; **24**:1552-1562.
11 Vander Heiden MG, Chandel NS, Williamson EK, Schumacker PT, Thompson CB. Bcl-xL regulates the membrane potential and volume homeostasis of mitochondria. *Cell* 1997; **91**:627-637.
12 Ekert PG, Read SH, Silke J, *et al.* Apaf-1 and caspase-9 accelerate apoptosis, but do not determine whether factor-deprived or drug-treated cells die. *J Cell Biol* 2004; **165**:835-842.
13 Broker LE, Kruyt FA, Giaccone G. Cell death independent of caspases: a review. *Clin Cancer Res* 2005; **11**:3155-3162.

14 Saelens X, Festjens N, Vande Walle L, van Gurp M, van Loo G, Vandenabeele P. Toxic proteins released from mitochondria in cell death. *Oncogene* 2004; **23**:2861-2874.
15 Jones JM, Datta P, Srinivasula SM, *et al.* Loss of Omi mitochondrial protease activity causes the neuromuscular disorder of mnd2 mutant mice. *Nature* 2003; **425**:721-727.
16 Martins LM, Morrison A, Klupsch K, *et al.* Neuroprotective role of the Reaper-related serine protease HtrA2/Omi revealed by targeted deletion in mice. *Mol Cell Biol* 2004; **24**:9848-9862.
17 Strauss KM, Martins LM, Plun-Favreau H, *et al.* Loss of function mutations in the gene encoding Omi/HtrA2 in Parkinson's disease. *Hum Mol Genet* 2005; **14**:2099-2111.
18 Hegde R, Srinivasula SM, Zhang Z, *et al.* Identification of Omi/HtrA2 as a mitochondrial apoptotic serine protease that disrupts inhibitor of apoptosis protein-caspase interaction. *J Biol Chem* 2002; **277**:432-438.
19 Martins LM, Iaccarino I, Tenev T, *et al.* The serine protease Omi/HtrA2 regulates apoptosis by binding XIAP through a reaper-like motif. *J Biol Chem* 2002; **277**:439-444.
20 Suzuki Y, Imai Y, Nakayama H, Takahashi K, Takio K, Takahashi R. A serine protease, HtrA2, is released from the mitochondria and interacts with XIAP, inducing cell death. *Mol Cell* 2001; **8**:613-621.
21 van Loo G, van Gurp M, Depuydt B, *et al.* The serine protease Omi/HtrA2 is released from mitochondria during apoptosis. Omi interacts with caspase-inhibitor XIAP and induces enhanced caspase activity. *Cell Death Differ* 2002; **9**:20-26.
22 Verhagen AM, Silke J, Ekert PG, *et al.* HtrA2 promotes cell death through its serine protease activity and its ability to antagonize inhibitor of apoptosis proteins. *J Biol Chem* 2002; **277**:445-454.
23 Yang QH, Church-Hajduk R, Ren J, Newton ML, Du C. Omi/HtrA2 catalytic cleavage of inhibitor of apoptosis (IAP) irreversibly inactivates IAPs and facilitates caspase activity in apoptosis. *Genes Dev* 2003; **17**:1487-1496.
24 Trencia A, Fiory F, Maitan MA, *et al.* Omi/HtrA2 promotes cell death by binding and degrading the anti-apoptotic protein ped/pea-15. *J Biol Chem* 2004; **279**:46566-46572.
25 Cilenti L, Soundarapandian MM, Kyriazis GA, *et al.* Regulation of HAX-1 anti-apoptotic protein by Omi/HtrA2 protease during cell death. *J Biol Chem* 2004; **279**:50295-50301.
26 Devin A, Lin Y, Liu ZG. The role of the death-domain kinase RIP in tumour-necrosis-factor-induced activation of mitogen-activated protein kinases. *EMBO Rep* 2003; **4**:623-627.
27 Yuasa T, Ohno S, Kehrl JH, Kyriakis JM. Tumor necrosis factor signaling to stress-activated protein kinase (SAPK)/Jun NH2-terminal kinase (JNK) and p38. Germinal center kinase couples TRAF2 to mitogen-activated protein kinase/ERK kinase kinase 1 and SAPK while receptor interacting protein associates with a mitogen-activated protein kinase kinase kinase upstream of MKK6 and p38. *J Biol Chem* 1998; **273**:22681-22692.
28 Walensky LD. BCL-2 in the crosshairs: tipping the balance of life and death. *Cell Death Differ* 2006; **13**:1339-1350.
29 Johnson DE. Regulation of survival pathways by IL-3 and induction of apoptosis following IL-3 withdrawal. *Front Biosci* 1998; **3**:d313-324.
30 Besancon F, Atfi A, Gespach C, Cayre YE, Bourgeade MF. Evidence for a role of NF-κB in the survival of hematopoietic cells mediated by interleukin 3 and the oncogenic TEL/platelet-derived growth factor receptor beta fusion protein. *Proc Natl Acad Sci USA* 1998; **95**:8081-8086.
31 Nakata S, Matsumura I, Tanaka H, *et al.* NF-κB family proteins participate in multiple steps of hematopoiesis through elimination of reactive oxygen species. *J Biol Chem* 2004; **279**:55578-55586.
32 Li CY, Zhan YQ, Xu CW, *et al.* EDAG regulates the proliferation and differentiation of hematopoietic cells and resists cell apoptosis through the activation of nuclear factor-κB. *Cell Death Differ* 2004; **11**:1299-1308.
33 Levkau B, Scatena M, Giachelli CM, Ross R, Raines EW. Apoptosis overrides survival signals through a caspase-mediated dominant-negative NF-κB loop. *Nat Cell Biol* 1999; **1**:227-233.
34 Nagata Y, Moriguchi T, Nishida E, Todokoro K. Activation of p38 MAP kinase pathway by erythropoietin and interleukin-3. *Blood* 1997; **90**:929-934.
35 Nagata Y, Nishida E, Todokoro K. Activation of JNK signaling pathway by erythropoietin, thrombopoietin, and interleukin-3. *Blood* 1997; **89**:2664-2669.
36 Baud V, Karin M. Signal transduction by tumor necrosis factor and its relatives. *Trends Cell Biol* 2001; **11**:372-377.
37 Kumar S, Boehm J, Lee JC. p38 MAP kinases: key signalling molecules as therapeutic targets for inflammatory diseases. *Nat Rev Drug Discov* 2003; **2**:717-726.
38 Yu C, Minemoto Y, Zhang J, *et al.* JNK suppresses apoptosis via phosphorylation of the proapoptotic Bcl-2 family protein BAD. *Mol Cell* 2004; **13**:329-340.
39 Vande Walle L, Van Damme P, Lamkanfi M, *et al.* Proteome-wide Identification of HtrA2/Omi Substrates. *J Proteome Res* 2007; **6**:1006-1015.
40 Vercammen D, Brouckaert G, Denecker G, *et al.* Dual signaling of the Fas receptor: initiation of both apoptotic and necrotic cell death pathways. *J Exp Med* 1998; **188**:919-930.
41 Cornelis S, Bruynooghe Y, Denecker G, Van Huffel S, Tinton S, Beyaert R. Identification and characterization of a novel cell cycle-regulated internal ribosome entry site. *Mol Cell* 2000; **5**:597-605.